energy&fuels

pubs.acs.org/EF

Article

Assessment of Kerogen Wettability from Contact Angle Goniometry

Murilo T. Suekuni, Mohammadamin Ezazi, Gibum Kwon, Paul R. Craddock, and Alan M. Allgeier*

Cite This: *Energy Fuels* 2024, 38, 1864−1872

Read Online

ACCESS | Metrics & More | Article Recommendations | Supporting Information

ABSTRACT: Understanding the wetting properties of shale reservoirs can benefit their development for energy-related purposes and their potential for long-term carbon dioxide injection and storage. Given its potential volumetric abundance and high surface area, the wetting behavior of kerogen in shale requires assessment. Despite their known limitations, wettability studies are commonly limited to static contact angle (θ) measurements. In this Article, the conflicting factors related to the analysis and interpretation of kerogen wetting via static contact angle measurements are discussed. Contact angle data for deionized water, brine (5% NaCl), and *n*-dodecane are presented for seven paleomarine type-II kerogens spanning a wide range of thermal maturities (vitrinite reflectance, R_o: 0.55 to 2.75%) and chemical composition (aromatic carbon content, H/C ratio, O/C ratio). Droplets of *n*-dodecane instantaneously absorbed ($\theta^* \approx 0°$) upon contact with all kerogen pellet surfaces, showing the oleophilic nature of kerogen for all maturities tested. Apparent contact angles of water with kerogen surfaces were positively correlated with H/C ratios and inversely correlated with aromatic carbon content, while the bulk and surface oxygen concentrations did not strongly correlate with the measured data. Kerogen exhibited hydrophobic ($\theta_{water} > 90°$) behavior, except at the highest thermal maturities. For example, the least thermally mature and most thermally mature samples studied presented apparent contact angles for water of 123 ± 15 and 59 ± 10°, respectively. Profilometry analyses showed roughness average values ranging from 0.4 ± 0.1 to 3.9 ± 0.7 μm, with the indication that sample topology can affect measured contact angles, albeit in second order as compared to sample chemistry in this study. We recommend caution when associating contact angle data alone with wetting behavior, as data obtained through sessile droplet analysis are subject to known but not always considered, caveats.

1. INTRODUCTION

Solid, insoluble organic matter (kerogen) dispersed in organic-rich mudrocks can host significant porosity and impact fluid flow in shale during fracturing and production.[1−3] Kerogen-fluid surface interactions can, therefore, impact petroleum production and water flowback in unconventional resource development, as well as the potential for geological CO_2 storage in organic-rich mudrocks (hereafter referred to as shale).[4,5] The complex composition and textural properties of shale, however, complicate efforts to quantify solid−fluid surface interactions, including kerogen wettability.[6]

Wettability is generally perceived as the tendency of a liquid to spread over a solid surface via adhesive and cohesive forces or to spontaneously imbibe via capillary forces.[7] Materials are classified as either wetting (-philic) or repelling (-phobic) with regards to a probe fluid.[8] In the context of oilfield reservoirs, wettability describes whether solid surfaces are preferentially in contact with water or petroleum or in some intermediate state (mixed-wet). The wetting state of conventional reservoir rocks applies only to surface interactions between liquid (water and/or oil) and minerals because the latter comprise the entire solid volume of the formation.[9,10] The wetting state of unconventional resources necessarily requires understanding the wetting properties of kerogen surfaces because of its volumetric importance in economic shale resources.[11,12]

Contact angle (θ) measurements are widely used for inferring surface wetting properties of solids, with applications in characterizing metal alloys, polymers, surface coatings, and membranes, as well as soils and sediments.[8,13−17] The sessile droplet method, while a convenient laboratory technique for measuring the contact angles, poses known challenges that can misguide the interpretation of solid surface wettability.[18] The observed contact angles may differ from the intrinsic contact angles and can be affected by testing conditions (e.g., temperature, droplet size, liquid evaporation), and surface conditions (e.g., contamination, roughness, porosity).[18−22] Several studies have examined the wetting properties of bulk shales.[4,23−29] General trends (e.g., versus total organic carbon [TOC] content, thermal maturity, liquid−gas composition of the sample), as well as inconsistencies (e.g., testing conditions), have been reviewed and discussed.[30,31] Generally, increasing oil imbibition in bulk shale with increasing organic matter content and thermal maturity suggests that kerogen is oil-wetting.[25,32] However, the wetting properties of kerogen in bulk rocks are confounded by the presence of minerals, which may exhibit different wetting behaviors with respect to the organic matter.

Despite the importance of kerogen in unconventional resources, there have been a limited number of contact angle studies of isolated kerogen. Yi and Lee recently presented contact angle data for aqueous solutions on isolated kerogen

Received: August 22, 2023
Revised: December 12, 2023
Accepted: December 14, 2023
Published: January 6, 2024

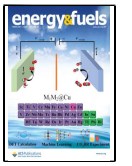

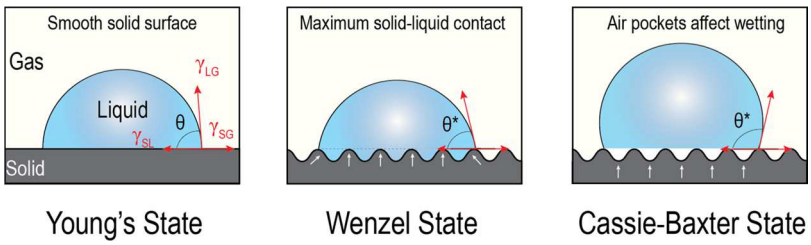

Figure 1. Schematic representation of the Young's, Wenzel, and Cassie−Baxter wetting states.

surfaces. However, their study focused on the alteration of wetting characteristics of kerogen induced by interaction and possible oxidation by hydraulic fracturing additives, and not on the wetting characteristics of pristine kerogen as addressed in the present study.[33] Jagadisan and Heidari reported contact angle data for isolated kerogen in air/water and air/oil, concluding that kerogen is "strongly hydrocarbon-wet at high thermal maturities and water-wet at low thermal maturities."[34] Their study of just two kerogen isolates was not referenced to the benchmark thermal maturity scale (i.e., vitrinite reflectance R_o, %) and relied on laboratory-simulated thermal proxies in assessing wettability trends. The primary mechanistic explanation for varying water-wetting behavior (i.e., abundance of polar versus nonpolar functionalities) does not adequately represent the trends demonstrated for the samples. For example, the kerogen sample with the highest O/C ratio did not exhibit the lowest contact angle, and the kerogen sample with similar aromatic contents exhibited very different contact angles. These results may indicate that a complex interplay of multiple variables determines the measured contact angles.

The wetting properties of kerogen were also investigated via molecular dynamics (MD) simulations. Hu et al., studied kerogen wettability with simulations of the idealized system of water or octane interacting with graphene sheets of varying contents of surface polar oxygen functionalities.[35] For such idealized surfaces, the contact angles of water on "kerogen" decreased with an increase in polar moieties (θ_{water} = 120° at O/C = 0.05; θ_{water} = 0° at O/C = 0.2). These results suggest that polar functional groups promote wettability. Other MD simulations have used more complex molecular models to represent kerogen, such as those developed by Ungerer et al.[36] Ho and Wang reported a simulated water contact angle of 43° on the surface of overmature type-II kerogen (Ungerer kerogen II-D model) in the CO_2/water/kerogen system at standard pressure.[37] Li et al., reported θ_{water} = 40 and 46° for the same kerogen II-D model.[38] These results are consistent with the experimental data obtained by Prydatko et al., who reported θ_{water} = 42° on graphene surfaces.[39] In contrast, Jagadisan and Heidari reported, for the same kerogen II-D model, θ_{water} = 76 and 89° in systems with air/water/kerogen and CO_2/water/kerogen, respectively.[40] Thus, ambiguity persists in our understanding of the wetting behavior of kerogen (and molecular proxies for kerogen).

In this study, we report water, brine, and *n*-dodecane contact angle measurements on surfaces of well-characterized kerogen isolates and addresses inconsistent results in previous studies. Our kerogens are diversely representative of paleomarine (type II) sedimentary organic matter and span across a wide range of thermal maturity from immature (R_o ~ 0.6%) to dry-gas stage (R_o ~ 2.8%). Noting that contact angle measurements can be impacted by compositional heterogeneity and surface roughness,[19,20,22] our contact angle data are evaluated against their wide range of chemical compositions and surface topography. Despite the limitation of the sessile-drop technique, our contact angle data provide the most direct evidence to date that kerogen is preferentially oil-wetting throughout the relevant range of thermal maturity.

1.1. Wettability Theory. Experimentally, contact angles (θ) under atmospheric conditions (room temperature and 1 atm pressure) are determined based on the tangential angle formed at the triphasic (gas−liquid−solid) interface.[16,41] Conventionally, contact angles for wetting fluids are <90°, whereas for nonwetting fluids ≥90°.[42,43] Regardless of its convenience, the outputs of static or advancing contact angle measurements should be considered cautiously since the observed behavior may be influenced by surface chemical heterogeneity, physical heterogeneity (e.g., topography), contamination (impurities), and testing conditions (e.g., pressure, temperature, droplet size, evaporation), among other factors.[20,44]

For ideal surfaces (i.e., topographically smooth, chemically homogeneous, and nonreactive), the Young's relation associates the measured contact angle (θ) at an equilibrium state with the interfacial tensions (or energies) at the solid−gas (γ_{SG}), solid−liquid (γ_{SL}), and liquid−gas (γ_{LG}) interfaces eq 1.[41,45]

$$\cos\theta = \frac{\gamma_{SG} - \gamma_{SL}}{\gamma_{LG}} \quad (1)$$

Under realistic conditions, most materials present certain surface roughness, affecting the interfacial contact area between the three phases, which limits the application of the Young's relation.[41] Ultimately, the wetting properties of a solid become a function of the surface chemistry and topography. In this case, the Wenzel and Cassie−Baxter relations can be used to account for these factors. In the Wenzel state of wettability, the liquid fully permeates the surface roughness, which enhances the wetting behavior in comparison to a smooth counterpart eq 2.[46]

$$\cos\theta^* = r\cos\theta \quad (2)$$

Here, the apparent contact angle (θ^*) for a liquid in the Wenzel wetting state is a function of the intrinsic contact angle (θ) and a surface roughness (r), characteristic of the ratio between the actual and projected surface areas (Figure 1).[46] Rough surfaces may also induce a wetting condition known as the Cassie−Baxter state of wettability.[47] In this state, air pockets are trapped between the liquid and the rough solid surface.[47,48] Accordingly, the apparent contact angle will be influenced by the fractional areas of the solid−liquid (f_{SL}) and liquid−gas (f_{LG}) interfaces, as expressed in eq 3.[47]

$$\cos\theta^* = f_{SL}\cos\theta - f_{LG} \quad (3)$$

https://doi.org/10.1021/acs.energyfuels.3c03175
Energy Fuels 2024, 38, 1864−1872

Table 1. Surface Roughness, Particle Size, and Contact Angle Data for Type-II Kerogen

formation name	R_o (%)	arithmetic average roughness, R_a (μm)	mean particle size, d_{50} (μm)	apparent contact angle		
				DI water, θ*	brine, θ*	n-dodecane, θ*
Jordanian oil shale	0.55	3.9 ± 0.6	91.0	123 ± 15°	123 ± 13°	0°
Eagle Ford	0.65	1.0 ± 0.1	40.7	105 ± 3°	109 ± 6°	0°
Bakken	0.95	0.7 ± 0.2	0.3	96 ± 1°	106 ± 5°	0°
Vaca Muerta (Argentina)	1.28	1.6 ± 0.8	14.5	92 ± 7°	106 ± 6°	0°
Vaca Muerta (Argentina)	1.61	0.4 ± 0.1	9.7	93 ± 1°	87 ± 3°	0°
Marcellus	2.20	2.0 ± 0.4	6.3	54 ± 7°	53°	0°
Woodford	2.75	0.4 ± 0.1	12.7	59 ± 10°	55 ± 5°	0°

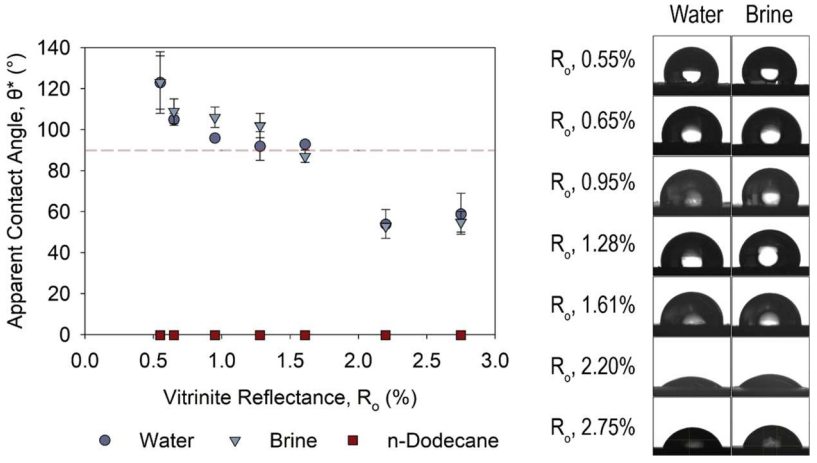

Figure 2. Contact angles of water, brine, and n-dodecane as a function of thermal maturity (left) and images of the contact angles of water and brine (right). The dashed line indicates the conventional hydrophobic wettability threshold (θ* = 90°).

A liquid in the Cassie–Baxter state can exhibit θ* > 90° even for θ < 90°. In practice, it is challenging to distinguish a liquid in the Wenzel state versus the Cassie–Baxter state. Figure 1 illustrates the above-described wetting states.[16,18,41]

2. EXPERIMENTAL SECTION

2.1. Kerogen Samples. The samples used in this study are seven type-II kerogen isolates obtained from paleomarine Bakken, Marcellus, Woodford, and Vaca Muerta Formations, described in earlier publications.[49−51] The kerogens span a wide range of thermal maturity from immature to dry-gas stage, as referenced by their vitrinite reflectance R_o values (0.55–2.75%).[49−51] The kerogens were isolated from bulk rock samples according to the best-practice conservative closed-system procedure, described elsewhere.[52,53] The kerogen isolates have been extensively analyzed for their bulk chemistry (elemental analysis), surface chemistry (X-ray photoelectron spectroscopy), molecular structure (solid-state ^{13}C nuclear magnetic resonance), and physical properties (grain density from gas pycnometry; pore surface area and pore volume from nitrogen physisorption), as recently compiled in Suekuni et al.,[54] and reported in Supporting Information, Table S1.

2.2. Particle Size Distribution. The particle size distributions of kerogen powders were measured via laser diffraction by using a Malvern Mastersizer 2000 in a range of 0.02 to 2000 μm according to ISO 13320:2020.[55] Samples were first wetted with isopropyl alcohol and mixed with 10 mL of a dilute (<0.1%) solution of sodium lauryl ether sulfate. Aliquots of the kerogen suspensions were pipetted into a disperser containing 150 mL of deionized water. The liquid media with suspended kerogen was continuously recirculated in the closed-loop system with simultaneous sonication for 20 s. The measurements assumed a refractive index of 1.60 + i0.012 at the helium–neon (HeNe) wavelength of 633 nm.[56]

2.3. Pellet Preparation. Approximately 350 mg of kerogen powder was gently ground by hand using a mortar and pestle to ensure the dispersion of particle aggregates. These powders were pressed into a pellet of diameter 24 mm and thickness 2 mm using a Wabash Hydraulic Press 12–10S at a pressure of 4000 psi for approximately 1 min (Figure S1).

2.4. Optical Profilometry. The surface roughness of the kerogen pellets was measured using a Veeco Wyko NT1100 Optical Profiler with a 10× objective lens in vertical scanning interferometry mode. Scans were collected over a rectangular area of approximately 450 μm × 600 μm (x and y directions, respectively) with a resolution of 0.9 μm in the transverse (x–y) plane and a vertical resolution of ∼1 Å, according to the equipment manufacturer. Uncertainty is reported as the standard deviation of 3–5 measurements on different regions of the pellet surface.

2.5. Contact Angle Measurements. The collection and interpretation of contact angle data by the sessile droplet technique have been discussed elsewhere.[16,18,41] Here, static contact angle measurements of three liquids, i.e., deionized (DI) water, brine (5% NaCl), and n-dodecane, on kerogen pellet surfaces were made using the sessile droplet method in a Ramé-Hart 190-U1 goniometer at room temperature (22 °C). Before contact angle measurements, all pellets were vacuum-dried at (<77 Torr) 60 °C for 6 h to remove moisture and contaminants while avoiding surface oxidation at higher temperatures.[57] Contact angles were measured 5 s after placing a 4 μL volume liquid drop on the pellet surface. Generally, triplicate measurements were carried out on different regions of each pellet surface. The uncertainty is reported as the standard deviation of the triplicate measurements. The datum reported without error bars was from a single measurement of brine on the surface of sample R_o = 2.20%. The Supporting Information contains a discussion of the method and interpretation of dynamic (i.e., advancing and receding) contact angle data.

3. RESULTS AND DISCUSSION

3.1. Apparent Contact Angles of Liquids on Kerogen Surfaces. Table 1 summarizes the measured contact angles θ*

https://doi.org/10.1021/acs.energyfuels.3c03175
Energy Fuels 2024, 38, 1864−1872

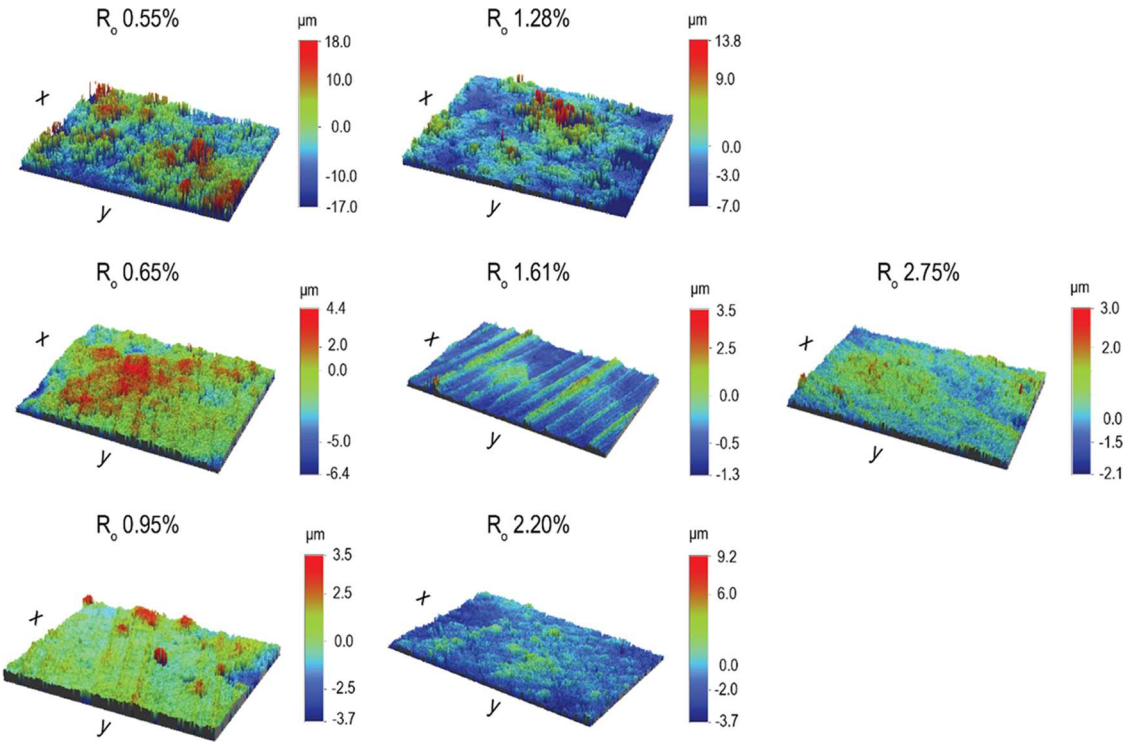

Figure 3. 3D maps of the kerogen pellet surfaces. The area of each map is approximately 450 μm × 600 μm.

for DI water, brine (5% NaCl), and *n*-dodecane on the surfaces of kerogen pellets. Figure 2 plots these apparent contact angles versus the thermal maturity (i.e., vitrinite reflectance R_o) of the kerogens together with static images of DI water and brine drops on the surface of the pellets. The data clearly support that kerogen is preferentially oil-wetting over the entire range of thermal maturities examined (immature to dry gas.)

The *n*-dodecane droplet nearly instantly wetted the entire kerogen surface and imbibed into the pellet, yielding contact angles of approximately zero. Finite ($\theta^* > 0°$) contact angles could not be measured for the liquid hydrocarbon; accordingly, no static images of *n*-dodecane on kerogen surfaces are shown in Figure 2. The Supporting Information contains video files illustrating the wetting of hydrocarbons and water on kerogen surfaces. Quantifying finite contact angles for liquids with low surface tension, including *n*-dodecane ($\gamma_{LG} \sim 25.4$ mN m^{-1}) is intrinsically challenging and mostly relies on the presence of repelling chemical or physical traits, such as surface roughness.[58−62]

Conversely, the examined kerogen surfaces were nearly all hydrophobic with respect to both DI water and brine, presenting apparent contact angles $\theta^* \geq 90°$ except at the highest thermal maturities examined ($\theta^* \sim 55°$; $R_o \geq 2.2\%$). The contact angles of brine were slightly higher than those measured for DI water, which is consistent with the higher surface tension of water in the presence of dissolved salts ($\gamma_{LG} \sim 75$ mN m^{-1} for NaCl-brine versus 72 mN m^{-1} for DI water, at room temperature).[63] However, we consider this difference between pure water and brine to be of second-order importance.

Spontaneous wetting and imbibition of hydrocarbons (e.g., *n*-decane, produced formation oil) have been reported on surfaces of bulk organic-rich mudrock samples under atmospheric conditions,[23,25,32] supporting our observations. Similarly, Yang et al. also reported higher contact angles for water on organic-rich mudrock samples of lower thermal maturity ($\theta^* \sim 21−62°$; $R_o \sim 1.1−1.6$) as compared to organic-rich mudrock samples of higher thermal maturity ($\theta^* \sim 3−17°$; $R_o \sim 2.2−3.1$), further supporting our observations.[23] In these previous studies, however, the presence of substantial mineral surfaces in bulk samples complicates the interpretation of the inherent wettability trends of organic matter.

3.2. Effects of Textural Properties on Contact Angles.

It is critical to determine whether the measured apparent contact angles θ^* are systematically impacted by textural properties like surface roughness and contact area, in addition to surface chemistry.[24] To the best of our knowledge, such analysis in consideration of kerogen wettability has not been performed. Surface topography maps obtained via optical profilometry show that the kerogen pellets present vertical heterogeneity within and between the samples, as is practically expected (Figure 3).

Table 1 summarizes the arithmetic average roughness (R_a) values of these surfaces, together with the mean particle size (d_{50}) of the samples obtained from laser diffraction analysis. The surface roughness R_a is the average of the surface height differentials from the mean height (baseline) and ranges from ∼0.4 to 3.9 μm. The R_a and d_{50} values are approximately positively correlated, suggesting that the solid particle size can influence the surface roughness. Thus, careful preparation of kerogen powders with particle size characterization is recommended for any wetting studies.

The data show a generally positive correlation between the apparent contact angle θ^* of water and brine on hydrophobic kerogen surfaces and the roughness R_a of that kerogen surface (Figure 4). The exception is sample R_o = 2.20%, which expresses a relatively large roughness (R_a = 2.0 μm) but a low apparent contact angle ($\theta^* \sim 55°$). Li et al., reported this same phenomenon for hydrophobic ($\theta^*_{water} > 90°$) coal (type-III

https://doi.org/10.1021/acs.energyfuels.3c03175
Energy Fuels 2024, 38, 1864−1872

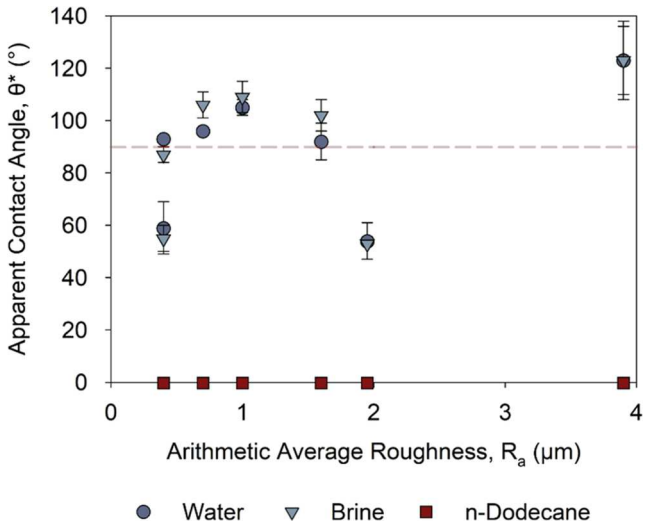

Figure 4. Apparent contact angle data as a function of the average surface roughness of kerogen pellets. The red dotted line in each figure marks the traditional demarcation of wetting/nonwetting behavior ($\theta^* = 90°$).

kerogen), where static θ^* of water decreased from ∼115 to ∼97° as surface roughness decreased.[22] However, a positive relationship between θ^* and the surface roughness is not always observed. Li et al., also showed that static θ^* of water increased on the surface of two hydrophilic ($\theta^*_{water} < 90°$) coals from ∼76 to ∼87 and ∼45 to ∼60° as surface their roughness was decreased.[22] Kozbial et al., similarly reported for graphite ($\theta^*_{water} < 90°$) that highly ordered pyrolytic graphite ($R_a \sim 0.3$ to 1.4 nm) presented a higher static θ^* compared to low-quality pyrolytic graphite ($R_a \sim 30$ nm).[20] Surface roughness appears to have only a second-order impact on static water/brine contact angles in our set of kerogen samples but seems to explain the relatively low contact angle of R_o = 2.20% compared to R_o = 2.75%. Notably, the former has a higher R_a, implying the nonideal Wenzel state of wetting. Importantly, surface roughness cannot explain the systematic and significant first-order difference between hydrocarbon and water-wetting behaviors on kerogen surfaces. Additional evaluations of the influence of surface roughness upon contact angles and contact angle hysteresis are presented in the Supporting Information.

3.3. Effects of Chemical Properties on Contact Angles. The wetting behavior of kerogen is now interpreted with respect to its bulk and surface chemical characteristics (Table S1). Figure 5 plots the apparent contact angle θ^* as a function of the bulk carbon aromaticity (%C_{arom}, from quantitative ^{13}C solid-state NMR), bulk atomic H/C ratio, bulk atomic O/C ratio, and surface oxygen concentration (O(1s), from X-ray photoelectron spectroscopy, XPS). Note that H/C and O/C are proxies for the abundance of aliphatic and oxygenated moieties, respectively.

Hydrocarbon (*n*-dodecane) instantly wetted kerogen surfaces ($\theta^* \approx 0°$), independent of kerogen's wide range of structural and chemical compositions. Apparent contact angles of water/brine on kerogen surfaces are positively correlated with hydrogen and—to a lesser degree, with oxygen content and inversely correlated with carbon aromaticity. Kerogen is hydrophobic for most kerogen structures except those nearly entirely aromatic (i.e., thermally mature kerogen with low H/C and O/C ratios). Lu et al., similarly described the decreasing water affinity on bulk shale surfaces (Qianjiang Formation, China) with increasing aliphatic chain length of organic matter

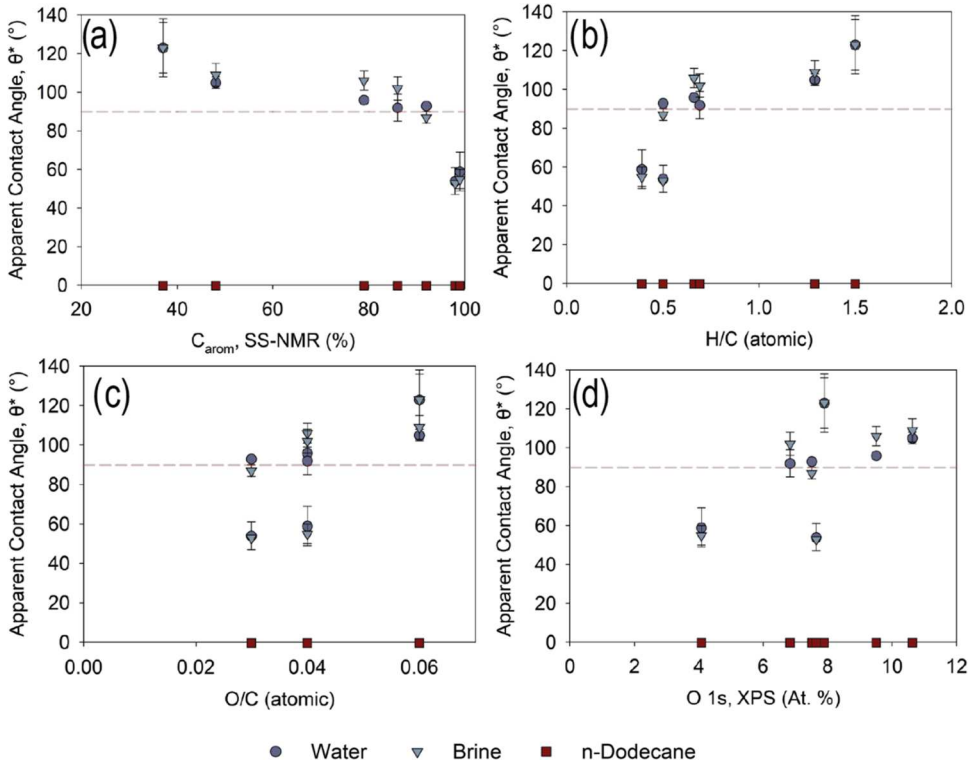

Figure 5. Contact angles of water, brine, and *n*-dodecane as a function of kerogen (a) aromatic content, (b) H/C ratios, (c) O/C ratios, and (d) surface atomic % of oxygen on the surface (XPS, O (1s) region). Note that the dashed lines mark 90°.

https://doi.org/10.1021/acs.energyfuels.3c03175
Energy Fuels 2024, 38, 1864−1872

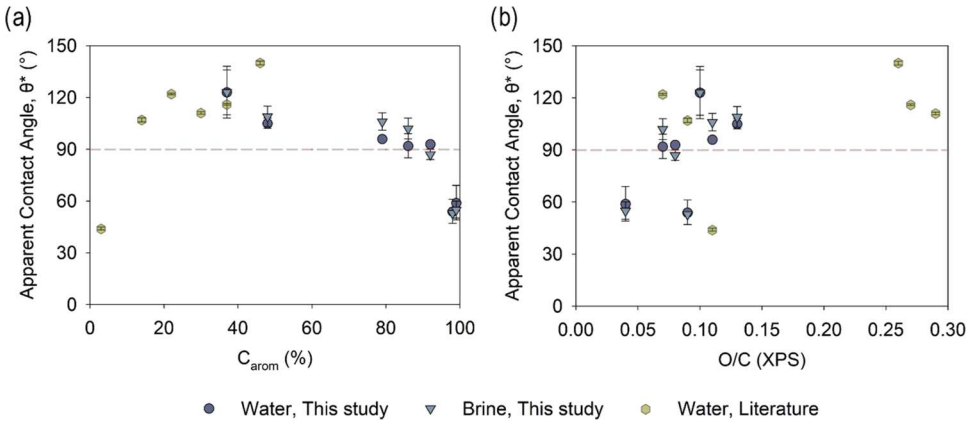

Figure 6. Water and brine (5% NaCl) apparent contact angles as a function of (a) aromatic content and (b) O/C ratio from this study and from literature.[34]

in the samples.[26] The water-wetting behavior of kerogen appears to be controlled by the relative amount of sp^2 (aromatic) versus sp^3 (aliphatic) carbon. Kerogen shows some affinity for polar water molecules only when its carbon structure is nearly entirely composed of polarizable sp^2 carbons. As an extreme, graphite and graphene, with their highly ordered and fully aromatic structures, also exhibit hydrophilic behavior.[20,37−39,44] The affinity of water and polarizable sp^2 carbons has similarly been suggested to explain the relative wetting behavior of the polymers poly(styrene) [PS] and poly(ethylene) [PE]. The PS, with a phenyl ring substituent on the backbone, is more polarizable than PE with no substituent on the backbone.[64] Correspondingly, PS has a higher solid surface energy and presents a lower contact angle for water.[64−67]

Figure 6 overlays literature contact angle data and data reported here for water on kerogen surfaces versus $\%C_{arom}$ and O/C.[34] A recent literature report concluded that kerogen is oleophobic/hydrophilic at low thermal maturity and hydrophobic at high thermal maturity.[34] A reinterpretation of this literature data is warranted with respect to the broader scope of kerogen data now available, which suggests that the determinants of kerogen wettability are more complex than previously described. For example, kerogen's hydrophobic behavior was attributed to increasing carbon aromaticity,[34] but the current more complete data set suggests, instead, that increasing carbon aromaticity results in weak hydrophilic behavior (Figure 6). This is explained by the higher polarizability of sp^2 (aromatic) carbons compared to sp^3 (aliphatic) carbons and is consistent with numerous literature reports characterizing graphite as hydrophilic.[20,39] The literature report also suggested that kerogen's hydrophilic behavior correlated positively with the abundance of polar oxygen.[34] This interpretation is not obviously supported by the larger set of data available now (Figure 6b). Indeed, the few kerogens in the literature with exceptionally high oxygen content (O/C ratios: 0.27−0.29) surprisingly showed hydrophobic behavior ($\theta^*_{water} > 90°$).[34] We note that such high O/C ratios are more characteristic of paleoterrestrial type-III kerogen than of typical paleomarine type-II kerogen,[68] which is acknowledged in the study. Otherwise, oxygen moieties do not appear to govern the wetting behavior of kerogen in typical paleomarine shales, most likely because of their low surface abundance generally (<3 atom %, Table S1).[69] Notably, the homogeneity of surface oxygen spatial distribution in these naturally occurring samples is not easily controlled and may contribute to variability in the data sets. Similarly, surface roughness, which was not reported for samples in the literature report,[34] may confound apparent measured contact angles. Finally, it was also acknowledged in that study that the removal of bitumen in synthetically matured samples leads to a decrease in the water contact angle even below 90°.

3.4. Implications for Wetting States in Shales.

Notwithstanding the challenges and limitations of the sessile droplet technique for interpreting the wetting properties of porous geomaterials, some implications for the wettability of organic-rich mudrocks are presented. The initial wetting state of bulk shale (i.e., before deep burial and generation of hydrocarbons from thermal cracking of kerogen[69,70]) is almost certainly water-wettable.[26,27] Formation water resides within mineral-hosted pore space, between and possibly within mineral grains (intergranular and intragranular porosity, respectively). Thermal cracking of kerogen first generates liquid hydrocarbons (oil window: $R_o \sim 0.6−1.35\%$).[71] These liquid hydrocarbons are generated within the so-called organic-hosted porosity that simultaneously develops within kerogen, as a direct result of thermal cracking processes. Within this range of thermal maturity, kerogen is evidently superoleophilic ($\theta^*_{oil} \sim 0°$) and hydrophobic ($\theta^*_{water} > 90°$). Thus, kerogen pores in liquid-bearing shales (e.g., tight-oil resources) are almost certainly oil-wetting, whereas the mineral-hosted pores are water-wetted unless displaced by the generated oil (a phenomenon not addressed in this study).

Continued thermal cracking of kerogen and of earlier-formed liquid hydrocarbons subsequently generates gas-phase hydrocarbons (wet-gas window: $R_o \sim 1.35−2.0\%$, and dry-gas window: $R_o > 2.0\%$).[71] These gaseous hydrocarbons are likewise generated within the so-called organic-hosted porosity but may also be generated within the mineral-hosted porosity if liquid hydrocarbon has previously been expelled from kerogen into the mineral matrix. Kerogen remains preferentially oil-wetting, although liquid hydrocarbons are not necessarily stable in situ within the shale resource. The weakly hydrophilic behavior of kerogen ($\theta^*_{water} > 50°$) within the dry-gas window ($R_o > 2.0\%$) implies that, in gas-shale resources, kerogen could be water-wet or mixed-wet in gas-shale resources, but only if water can displace low-molecular-weight hydrocarbon gases from kerogen pore surfaces.

Further interpretation of shale wettability and fluid-flow dynamics within organic-hosted and mineral-hosted pores in

https://doi.org/10.1021/acs.energyfuels.3c03175
Energy Fuels 2024, 38, 1864−1872

shale requires additional and integrated measurements and modeling via, e.g., Washburn capillary rise, dynamic core-flooding, and captive bubble techniques.[25,39,72]

4. CONCLUSIONS

Unveiling the controlling factors of mixed-fluid dynamics in shale resources is beneficial for the efficient extraction of liquid and gas hydrocarbons as well as for possible injection of CO_2 for long-term geological storage. However, experimental determination of reservoir wetting properties is not straightforward, and controlling factors and trends are debatable. Kerogen is evidenced to be consistently and highly oleophilic for a wide range of thermal maturities (vitrinite reflectance R_o) and related chemical compositions (e.g., bulk $\%C_{arom}$, atomic H/C, and atomic O/C) as demonstrated by spontaneous imbibition of liquid hydrocarbon (*n*-dodecane) on kerogen surfaces. Likewise, the kerogens are hydrophobic or are weakly hydrophilic only for kerogen structures nearly entirely aromatic in carbon moieties. The latter observation is consistent with experimental measurements of water contact angles on graphitic surfaces and molecular dynamics simulations using in-silico kerogen models. Our study shows that characterizing shale wettability solely by the sessile droplet method may lead to incorrect conclusions. Evaluation of surface roughness is warranted in assessing contact angle data, though in the present study, surface roughness was of secondary importance compared to sample composition. Complementary future research efforts involving the wetting properties of kerogen or other materials are encouraged to integrate chemical and textural analysis into data interpretation, and are necessary to fully understand how differential wetting behavior of organic (kerogen) and inorganic (mineral) phases in complex geological formations impacts the flow of fluids within these reservoirs.

■ ASSOCIATED CONTENT

Supporting Information

The Supporting Information is available free of charge at https://pubs.acs.org/doi/10.1021/acs.energyfuels.3c03175.

Select bulk properties and dynamic contact angle data of type II kerogen (XLSX)

Kerogen pellet; list of formation names; elemental analysis; $\%C_{arom}$ (^{13}C NMR); atom % O(1s) (XPS); specific surface area and total pore volume (N_2 physisorption); advancing and receding contact angle, and contact angle hysteresis data (PDF)

Contact angle measurements of *n*-dodecane on sample R_o 2.8% (MP4)

Contact angle measurements of water on sample R_o 2.8% (MP4)

■ AUTHOR INFORMATION

Corresponding Author

Alan M. Allgeier − *Department of Chemical and Petroleum Engineering, The Center for Environmentally Beneficial Catalysis, and The Institute for Sustainable Engineering, University of Kansas, Lawrence, Kansas 66045, United States;* orcid.org/0000-0001-9122-2108; Email: alan.allgeier@ku.edu

Authors

Murilo T. Suekuni − *Department of Chemical and Petroleum Engineering, The Center for Environmentally Beneficial Catalysis, and The Institute for Sustainable Engineering, University of Kansas, Lawrence, Kansas 66045, United States;* orcid.org/0000-0003-1558-6780

Mohammadamin Ezazi − *Department of Mechanical Engineering, Georgia Southern University, Statesboro, Georgia 30460, United States*

Gibum Kwon − *Department of Mechanical Engineering, University of Kansas, Lawrence, Kansas 66045, United States;* orcid.org/0000-0002-7192-1910

Paul R. Craddock − *Schlumberger-Doll Research Center, Cambridge, Massachusetts 02139, United States;* orcid.org/0000-0003-4702-0204

Complete contact information is available at: https://pubs.acs.org/10.1021/acs.energyfuels.3c03175

Notes

The authors declare no competing financial interest.

■ ACKNOWLEDGMENTS

The authors acknowledge the financial support from the American Chemical Society−Petroleum Research Funds (ACS-PRF) grant (61103-ND10). Gibum Kwon thanks the National Science Foundation for financial support under grant CBET-1944314. Murilo T. Suekuni and Alan M. Allgeier thank Dr. Anoop Uchagawkar for the assistance with pellet preparation and Dr. David Scott at Particle at Advanced Particle Sensor, LLC for the particle size analysis of kerogen. The authors thank the following persons for sharing mudrock samples used in our study: Carolina Bernhardt (YPF S.A.), L. Taras Bryndzia, and Ronny Hofmann (through the X-Shale project, a joint industry-academic R&D collaboration between Shell-MIT-SLB), and Brian Cardott (Oklahoma Geological Survey).

■ REFERENCES

(1) Collell, J.; Galliero, G.; Vermorel, R.; Ungerer, P.; Yiannourakou, M.; Montel, F.; Pujol, M. Transport of Multicomponent Hydrocarbon Mixtures in Shale Organic Matter by Molecular Simulations. *J. Phys. Chem. C* **2015**, *119* (39), 22587−22595.

(2) Vasileiadis, M.; Peristeras, L. D.; Papavasileiou, K. D.; Economou, I. G. Transport Properties of Shale Gas in Relation to Kerogen Porosity. *J. Phys. Chem. C* **2018**, *122* (11), 6166−6177.

(3) Craddock, P. R.; Haecker, A.; Bake, K. D.; Pomerantz, A. E. Universal Curves Describing the Chemical and Physical Evolution of Type II Kerogen during Thermal Maturation. *Energy Fuels* **2020**, *34* (12), 15217−15233.

(4) Guiltinan, E. J.; Cardenas, M. B.; Bennett, P. C.; Zhang, T.; Espinoza, D. N. The Effect of Organic Matter and Thermal Maturity on the Wettability of Supercritical CO2 on Organic Shales. *Int. J. Greenhouse Gas Control* **2017**, *65*, 15−22.

(5) Hu, Y.; Devegowda, D.; Striolo, A.; Phan, A.; Ho, T. A.; Civan, F.; Sigal, R. The Dynamics of Hydraulic Fracture Water Confined in Nano-Pores in Shale Reservoirs. *J. Unconv. Oil Gas Resour.* **2015**, *9*, 31−39.

(6) AlRatrout, A.; Blunt, M. J.; Bijeljic, B. Wettability in Complex Porous Materials, the Mixed-Wet State, and Its Relationship to Surface Roughness. *Proc. Natl. Acad. Sci. U.S.A.* **2018**, *115* (36), 8901−8906.

(7) Extrand, C. W. Origins of Wetting. *Langmuir* **2016**, *32* (31), 7697−7706.

(8) Shrestha, B.; Ezazi, M.; Kwon, G. Engineered Nanoparticles with Decoupled Photocatalysis and Wettability for Membrane-Based

Desalination and Separation of Oil-Saline Water Mixtures. *Nanomaterials* **2021**, *11* (6), No. 1397.
(9) Iglauer, S. CO_2 − Water−Rock Wettability: Variability, Influencing Factors, and Implications for CO_2 Geostorage. *Acc. Chem. Res.* **2017**, *50* (5), 1134−1142.
(10) Botto, J.; Fuchs, S. J.; Fouke, B. W.; Clarens, A. F.; Freiburg, J. T.; Berger, P. M.; Werth, C. J. Effects of Mineral Surface Properties on Supercritical CO_2 Wettability in a Siliciclastic Reservoir. *Energy Fuels* **2017**, *31* (5), 5275−5285.
(11) King, H. E.; Eberle, A. P. R.; Walters, C. C.; Kliewer, C. E.; Ertas, D.; Huynh, C. Pore Architecture and Connectivity in Gas Shale. *Energy Fuels* **2015**, *29* (3), 1375−1390.
(12) Chalmers, G. R.; Bustin, R. M.; Power, I. M. Characterization of Gas Shale Pore Systems by Porosimetry, Pycnometry, Surface Area, and Field Emission Scanning Electron Microscopy/Transmission Electron Microscopy Image Analyses: Examples from the Barnett, Woodford, Haynesville, Marcellus, and Doig Units. *AAPG Bull.* **2012**, *96* (6), 1099−1119.
(13) Kubiak, K. J.; Wilson, M. C. T.; Mathia, T. G.; Carval, P. Wettability versus Roughness of Engineering Surfaces. *Wear* **2011**, *271* (3−4), 523−528.
(14) Grundke, K.; Pöschel, K.; Synytska, A.; Frenzel, R.; Drechsler, A.; Nitschke, M.; Cordeiro, A. L.; Uhlmann, P.; Welzel, P. B. Experimental Studies of Contact Angle Hysteresis Phenomena on Polymer Surfaces — Toward the Understanding and Control of Wettability for Different Applications. *Adv. Colloid Interface Sci.* **2015**, *222*, 350−376.
(15) Ojeda, G.; Mattana, S.; Àvila, A.; Alcañiz, J. M.; Volkmann, M.; Bachmann, J. Are Soil−Water Functions Affected by Biochar Application? *Geoderma* **2015**, *249*−*250*, 1−11.
(16) Kwok, D. Y.; Neumann, A. W. Contact Angle Measurement and Contact Angle Interpretation. *Adv. Colloid Interface Sci.* **1999**, *81* (3), 167−249.
(17) Shrestha, B.; Ezazi, M.; Ajayan, S.; Kwon, G. Reversible Adsorption and Desorption of PFAS on Inexpensive Graphite Adsorbents *via* Alternating Electric Field. *RSC Adv.* **2021**, *11* (55), 34652−34659.
(18) Kung, C. H.; Sow, P. K.; Zahiri, B.; Mérida, W. Assessment and Interpretation of Surface Wettability Based on Sessile Droplet Contact Angle Measurement: Challenges and Opportunities. *Adv. Mater. Interfaces* **2019**, *6* (18), No. 1900839.
(19) Krainer, S.; Hirn, U. Contact Angle Measurement on Porous Substrates: Effect of Liquid Absorption and Drop Size. *Colloids Surf., A* **2021**, *619*, No. 126503.
(20) Kozbial, A.; Trouba, C.; Liu, H.; Li, L. Characterization of the Intrinsic Water Wettability of Graphite Using Contact Angle Measurements: Effect of Defects on Static and Dynamic Contact Angles. *Langmuir* **2017**, *33* (4), 959−967.
(21) Lößlein, S. M.; Merz, R.; Müller, D. W.; Kopnarski, M.; Mücklich, F. An In-Depth Evaluation of Sample and Measurement Induced Influences on Static Contact Angle Measurements. *Sci. Rep.* **2022**, *12* (1), No. 19389.
(22) Li, C.; Zhang, J.; Han, J.; Yao, B. A Numerical Solution to the Effects of Surface Roughness on Water−Coal Contact Angle. *Sci. Rep.* **2021**, *11* (1), No. 459.
(23) Yang, R.; He, S.; Hu, Q.; Zhai, G.; Yi, J.; Zhang, L. Comparative Investigations on Wettability of Typical Marine, Continental, and Transitional Shales in the Middle Yangtze Platform (China). *Energy Fuels* **2018**, *32* (12), 12187−12197.
(24) Sadeghinezhad, E.; Siddiqui, M. A. Q.; Roshan, H.; Regenauer-Lieb, K. On the Interpretation of Contact Angle for Geomaterial Wettability: Contact Area versus Three-Phase Contact Line. *J. Pet. Sci. Eng.* **2020**, *195*, No. 107579.
(25) Yassin, M. R.; Begum, M.; Dehghanpour, H. Organic Shale Wettability and Its Relationship to Other Petrophysical Properties: A Duvernay Case Study. *Int. J. Coal Geol.* **2017**, *169*, 74−91.
(26) Lu, Y.; Tian, R.; Tang, J.; Jia, Y.; Lu, Z.; Sun, X. Investigating the Mineralogical and Chemical Effects of CO_2 Injection on Shale Wettability at Different Reservoir Temperatures and Pressures. *Energy Fuels* **2021**, *35* (18), 14838−14851.
(27) Yuan, Y.; Rezaee, R.; Zou, J.; Liu, K. Pore-Scale Study of the Wetting Behavior in Shale, Isolated Kerogen, and Pure Clay. *Energy Fuels* **2021**, *35* (22), 18459−18466.
(28) Lu, Y.; Zeng, L.; Sari, A.; Chen, Y.; Jin, Y.; Xie, Q. Wetting Behavior of Shale Rocks and Its Relationship to Oil Composition. *Energy Fuels* **2019**, *33* (12), 12270−12277.
(29) Gosiewska, A.; Drelich, J.; Laskowski, J. S.; Pawlik, M. Mineral Matter Distribution on Coal Surface and Its Effect on Coal Wettability. *J. Colloid Interface Sci.* **2002**, *247* (1), 107−116.
(30) Siddiqui, M. A. Q.; Ali, S.; Fei, H.; Roshan, H. Current Understanding of Shale Wettability: A Review on Contact Angle Measurements. *Earth-Sci. Rev.* **2018**, *181*, 1−11.
(31) Arif, M.; Zhang, Y.; Iglauer, S. Shale Wettability: Data Sets, Challenges, and Outlook. *Energy Fuels* **2021**, *35* (4), 2965−2980.
(32) Begum, M.; Yassin, M. R.; Dehghanpour, H. Effect of Kerogen Maturity on Organic Shale Wettability: A Duvernay Case Study. *Mar. Pet. Geol.* **2019**, *110*, 483−496.
(33) Yi, X.; Lee, K. J. In *Wettability Alteration of Kerogen by Interacting with Hydraulic Fracturing Fluid*, SPE Annual Technical Conference and Exhibition; SPE: Houston, Texas, USA, 2022.
(34) Jagadisan, A.; Heidari, Z. Experimental Quantification of the Effect of Thermal Maturity of Kerogen on Its Wettability. *SPE Reservoir Eval. Eng.* **2019**, *22* (04), 1323−1333.
(35) Hu, Y.; Devegowda, D.; Sigal, R. A Microscopic Characterization of Wettability in Shale Kerogen with Varying Maturity Levels. *J. Nat. Gas Sci. Eng.* **2016**, *33*, 1078−1086.
(36) Ungerer, P.; Collell, J.; Yiannourakou, M. Molecular Modeling of the Volumetric and Thermodynamic Properties of Kerogen: Influence of Organic Type and Maturity. *Energy Fuels* **2015**, *29* (1), 91−105.
(37) Ho, T. A.; Wang, Y. Molecular Origin of Wettability Alteration of Subsurface Porous Media upon Gas Pressure Variations. *ACS Appl. Mater. Interfaces* **2021**, *13* (34), 41330−41338.
(38) Li, W.; Zhang, M.; Nan, Y.; Pang, W.; Jin, Z. Molecular Dynamics Study on CO_2 Storage in Water-Filled Kerogen Nanopores in Shale Reservoirs: Effects of Kerogen Maturity and Pore Size. *Langmuir* **2021**, *37* (1), 542−552.
(39) Prydatko, A. V.; Belyaeva, L. A.; Jiang, L.; Lima, L. M. C.; Schneider, G. F. Contact Angle Measurement of Free-Standing Square-Millimeter Single-Layer Graphene. *Nat. Commun.* **2018**, *9* (1), No. 4185.
(40) Jagadisan, A.; Heidari, Z. Molecular Dynamic Simulation of the Impact of Thermal Maturity and Reservoir Temperature on the Contact Angle and Wettability of Kerogen. *Fuel* **2022**, *309*, No. 122039.
(41) Marmur, A. Soft Contact: Measurement and Interpretation of Contact Angles. *Soft Matter* **2006**, *2* (1), 12−17.
(42) Blossey, R. Self-Cleaning Surfaces—Virtual Realities. *Nat. Mater.* **2003**, *2* (5), 301−306.
(43) Verplanck, N.; Coffinier, Y.; Thomy, V.; Boukherroub, R. Wettability Switching Techniques on Superhydrophobic Surfaces. *Nanoscale Res. Lett.* **2007**, *2* (12), No. 577.
(44) Amadei, C. A.; Lai, C.-Y.; Heskes, D.; Chiesa, M. Time Dependent Wettability of Graphite upon Ambient Exposure: The Role of Water Adsorption. *J. Chem. Phys.* **2014**, *141* (8), No. 084709.
(45) de Gennes, P. G. Wetting: Statics and Dynamics. *Rev. Mod. Phys.* **1985**, *57* (3), 827−863.
(46) Wenzel, R. N. Resistance of Solid Surfaces to Wetting by Water. *Ind. Eng. Chem.* **1936**, *28* (8), 988−994.
(47) Cassie, A. B. D.; Baxter, S. Wettability of Porous Surfaces. *Trans. Faraday Soc.* **1944**, *40*, 546−551.
(48) Liu, J.-L.; Feng, X.-Q.; Wang, G.; Yu, S.-W. Mechanisms of Superhydrophobicity on Hydrophilic Substrates. *J. Phys.: Condens. Matter* **2007**, *19* (35), No. 356002.
(49) Mukhopadhyay, P. K. Maturation of Organic Matter as Revealed by Microscopic Methods: Applications and Limitations of Vitrinite Reflectance, and Continuous Spectral and Pulsed Laser

https://doi.org/10.1021/acs.energyfuels.3c03175
Energy Fuels 2024, 38, 1864−1872

Fluorescence Spectroscopy. In *Developments in Sedimentology*; Wolf, K. H.; Chilingarian, G. V., Eds.; Elsevier, 1992; Vol. *47*, pp 435−510.
(50) Hackley, P. C.; Araujo, C. V.; Borrego, A. G.; Bouzinos, A.; Cardott, B. J.; Cook, A. C.; Eble, C.; Flores, D.; Gentzis, T.; Gonçalves, P. A.; et al. Standardization of Reflectance Measurements in Dispersed Organic Matter: Results of an Exercise to Improve Interlaboratory Agreement. *Mar. Pet. Geol.* **2015**, *59*, 22−34.
(51) Hackley, P. C. Application of Organic Petrology in High Maturity Shale Gas Systems. In *The Role of Organic Petrology in the Exploration of Conventional and Unconventional Hydrocarbon Systems*; Suárez-Ruiz, I.; Mendonça Filho, J. G., Eds.; Bentham Science Publishers: Sharjah, U.A.E, 2017; pp 206−236.
(52) Pernia, D. Application and Assessment of Open-System vs. Closed-System Kerogen Isolation Methods for Characterization of Gas Shale Kerogens, M.S. Thesis; University of Houston: Houston, TX, 2012.
(53) Ibrahimov, R. A.; Bissada, K. K. A. Comparative Analysis and Geological Significance of Kerogen Isolated Using Open-System (Palynological) versus Chemically and Volumetrically Conservative Closed-System Methods. *Org. Geochem.* **2010**, *41* (8), 800−811.
(54) Suekuni, M. T.; Craddock, P. R.; Douglas, J. T.; Pomerantz, A. E.; Allgeier, A. M. Critical Practices for the Preparation and Analysis of Kerogen. *Energy Fuels* **2022**, *36* (16), 8828−8843.
(55) International Organization for Standardization. ISO 13320:2020(E) Particle Size Analysis — Laser Diffraction Methods, 2020.
(56) Khare, B. N.; Thompson, W. R.; Sagan, C.; Arakawa, E. T.; Meisse, C.; Gilmour, I. Optical Constants of Kerogen from 0.15 to 40 μM: Comparison with Meteoritic Organics. In *Origin and Evolution of Interplanetary Dust*; Levasseur-Regourd, A. C.; Hasegawa, H., Eds.; Springer Netherlands: Dordrecht, 1991; pp 99−101.
(57) Durand, B.; Nicaise, G. Procedures for Kerogen Isolation. In *Kerogen—Insoluble Organic Matter from Sedimentary Rocks*; Durand, B., Ed.; Editions Technip: Paris, 1980; pp 35−53.
(58) Li, D.; Neumann, A. W. Contact Angles on Hydrophobic Solid Surfaces and Their Interpretation. *J. Colloid Interface Sci.* **1992**, *148* (1), 190−200.
(59) Tuteja, A.; Choi, W.; Ma, M.; Mabry, J. M.; Mazzella, S. A.; Rutledge, G. C.; McKinley, G. H.; Cohen, R. E. Designing Superoleophobic Surfaces. *Science* **2007**, *318* (5856), 1618−1622.
(60) Aulin, C.; Yun, S. H.; Wågberg, L.; Lindström, T. Design of Highly Oleophobic Cellulose Surfaces from Structured Silicon Templates. *ACS Appl. Mater. Interfaces* **2009**, *1* (11), 2443−2452.
(61) Kota, A. K.; Kwon, G.; Tuteja, A. The Design and Applications of Superomniphobic Surfaces. *NPG Asia Mater.* **2014**, *6* (7), e109.
(62) Kwon, G.; Kota, A. K.; Li, Y.; Sohani, A.; Mabry, J. M.; Tuteja, A. On-Demand Separation of Oil-Water Mixtures. *Adv. Mater.* **2012**, *24* (27), 3666−3671.
(63) Nasr-El-Din, H. A. In *Surface Tension of Completion Brines*, SPE International Symposium on Oilfield Chemistry; Society of Petroleum Engineers: Houston, Texas, USA, 2005.
(64) Graziano, G. Aliphatics vs. Aromatics Hydration Thermodynamics. *Biophys. Chem.* **2004**, *110* (3), 249−258.
(65) Petke, F. D.; Ray, B. R. Temperature Dependence of Contact Angles of Liquids on Polymeric Solids. *J. Colloid Interface Sci.* **1969**, *31* (2), 216−227.
(66) Ellison, A. H.; Zisman, W. A. Wettability Studies on Nylon, Polyethylene Terephthalate and Polystyrene. *J. Phys. Chem. A* **1954**, *58* (6), 503−506.
(67) Fowkes, F. M. Attractive Forces at Interfaces. *Ind. Eng. Chem.* **1964**, *56* (12), 40−52.
(68) Van Krevelen, D. W. Organic Geochemistry—Old and New. *Org. Geochem.* **1984**, *6*, 1−10.
(69) Vandenbroucke, M.; Largeau, C. Kerogen Origin, Evolution and Structure. *Org. Geochem.* **2007**, *38* (5), 719−833.
(70) Durand, B. Sedimentary Organic Matter and Kerogen. Definition and Quantitative Importance of Kerogen. In *Kerogen—Insoluble Organic Matter from Sedimentary Rocks*; Éditions Technip: Paris, France, 1980; pp 13−34.
(71) Dembicki, H. Three Common Source Rock Evaluation Errors Made by Geologists during Prospect or Play Appraisals. *AAPG Bull.* **2009**, *93* (3), 341−356.
(72) Jaine, J. E.; Mucalo, M. R. Measurements of the Wettability of Catalyst Support Materials Using the Washburn Capillary Rise Technique. *Powder Technol.* **2015**, *276*, 123−128.

https://doi.org/10.1021/acs.energyfuels.3c03175
Energy Fuels 2024, 38, 1864−1872